

Probing very slow $H^+ + D(1s)$ collisions using the ground-state dissociation of HD^+

E. Wells,* K. D. Carnes, and I. Ben-Itzhak

J. R. Macdonald Laboratory, Department of Physics, Kansas State University, Manhattan, Kansas 66506-2604

(Received 31 October 2002; published 18 March 2003)

Sub-eV collisions between protons and atomic deuterium targets are studied by utilizing the very slow dissociation of HD^+ from its electronic ground state. Studying the resulting $H^+ + D(1s)$ “half” collisions accesses energies more than an order of magnitude lower, and with better energy resolution, than previous measurements. The collision energy is determined *a posteriori* via three-dimensional momentum imaging. New results for energies near the threshold for charge transfer, incorporating an improved approach to the key problem of subtracting the H_2^+ background, are presented along with a discussion of the experimental technique.

DOI: 10.1103/PhysRevA.67.032708

PACS number(s): 34.50.Gb

I. INTRODUCTION

The dominant charge changing reaction in slow ion-atom collisions is charge transfer, and therefore understanding this reaction is a key part of investigations of plasma environments ranging from tokamaks and cold plasma processing to planetary atmospheres and interstellar clouds [1–5]. A proton colliding with a hydrogen atom in the electronic ground state is, in turn, the most basic ion-atom collision system for examination of the charge-transfer mechanism. These fundamental three-body collisions have been investigated theoretically at least since the 1953 semiclassical calculation of Dalgarno and Yadav [6]. Experimental examination has also been extensive, as discussed by Gilbody in his review [7].

The heteronuclear $H^+ + D(1s)$ collision system, though electronically similar to the $H^+ + H(1s)$ system described above, differs from it in two significant respects. First, the different nuclear masses lead to experimentally distinguishable final products, enabling experiments to probe this system at lower energies [7,8]. More importantly, the difference in nuclear mass breaks the symmetry under nuclear exchange and creates a small energy gap between the lowest two electronic states of the transient HD^+ . Thus, charge transfer in the $H^+ + D(1s)$ system is only a near resonant process. This difference is significant, since calculations of the HD^+ potential must go beyond a strict Born-Oppenheimer approach to address the fact that the center of mass and the center of charge are not located in the same place for this system [9–17]. The isotopic splitting of the lowest two HD^+ electronic states is illustrated in Fig. 1. The $H^+ + D(1s)$ collision system is frequently used as a test case by theorists seeking different approaches to the problem of electron translation factors for scattering calculations within the molecular orbital framework [9–11,14,16,17]. At very slow collision velocities, these translation factors can give rise to certain “spurious couplings” in some calculations [11], the origins of which are still a source of some controversy [16,18]. In addition, the $H^+ + D(1s)$ system has specific applications in atmospheric physics, where it helps regulate the escape of

hydrogen from planetary atmospheres [3], and astrophysics, where it is an important step in the creation of several deuterated molecules [5,19–21].

Theoretical interest in the $H^+ + D(1s)$ collision system is highest at energies lower than 1 eV, since most of the isotopic effects disappear at higher energies [11]. Most experiments, however, have been done at collision energies above 10 eV [7]. Using a traditional merged-beams approach to obtain experimental results at these low energies is difficult, since the relative velocity of the neutral and ion beams must be controlled very precisely. Newman and co-workers [8] were able to measure charge transfer in the $H^+ + D(1s)$ system down to 120_{-30}^{+48} meV. While a remarkable achievement for a merged-beam experiment, the energy resolution of that experiment was still insufficient to probe theory in a stringent way.

We have recently reported measurements of charge transfer and elastic scattering using a new method that does not suffer from the limitations of the merged-beams technique [22]. In this technique, the dissociation of HD^+ molecular ions in the vibrational continuum of the electronic ground

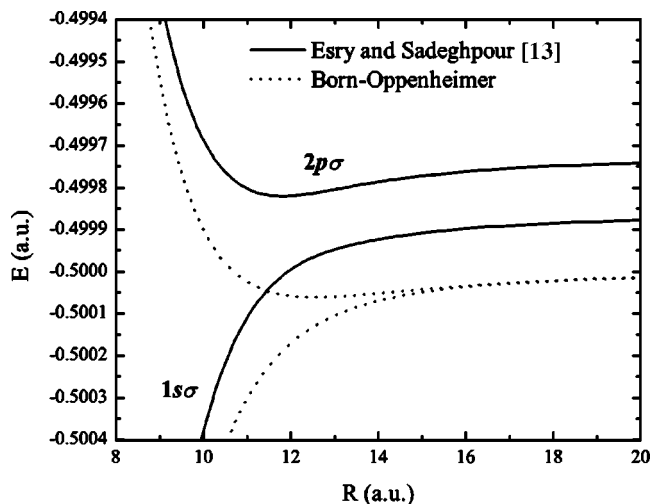


FIG. 1. The ground and first-excited HD^+ potential-energy curves, calculated by Esry and Sadeghpour [13] showing the isotopic splitting of the energy levels and the shift from the Born-Oppenheimer calculations.

*Present address: Department of Physics, University of Virginia, Charlottesville, VA 22904-4714.

state is used to produce very slow $H^+ + D(1s)$ “half” collisions. In a half collision, the dissociating fragments, $H^+ + D(1s)$, evolve from the internuclear separation at the time of the ionization, $R \approx R_0$, to $R = \infty$. The difference between these half collisions and traditional “full” collisions is that during the half collision, the range of internuclear distances is traversed only once. Charge transfer can occur during the dissociation process, most likely near $R = 12$ a.u., where the coupling is strongest [17]. Experimentally, the signature of a charge-transfer event is the detection of a very slow D^+ ion, while elastic scattering is associated with a H^+ ion. The collision energy is determined by measuring the vector momentum of the low-energy charged fragment produced in the ground-state dissociation process. In essence, the dissociating molecule is used as an accelerator for the investigation of this fundamental very low-energy charge-transfer process. Furthermore, it enables studies of elastic scattering, an interesting reaction channel at low energies, that cannot be measured using merged-beam techniques.

In this paper we present, in detail, this experimental method and examine its limitations. New results for the charge-transfer channel, reflecting a modified approach to the subtraction of the H_2^+ contamination from the measurement, are presented. The new data extend the range of the experiment almost down to the 3.7 meV threshold of charge transfer. The ultimate experimental limit with this technique is examined using a simulation. In addition, we suggest how this dissociation channel can be used as a sensitive probe of molecular alignment and momentum transfer in ion-molecule collisions.

II. EXPERIMENTAL METHOD

As described previously [22–24], and illustrated in Fig. 2, the “ground-state dissociation” (GSD) process is initiated by single ionization of a neutral HD target by a fast (usually 4 MeV) proton. The resulting vertical ionization, which is described very well by the Franck-Condon approximation, populates the vibrational continuum of the $HD^+(1s\sigma)$ state $1.0040\% \pm 0.0008\%$ of the time relative to the dominant nondissociative single-ionization channel [23]. The $HD^+(1s\sigma)$ state then dissociates into $H^+ + D(1s)$, which can potentially undergo a charge-transfer reaction, as described in the Introduction. The probability of a GSD event occurring as a function of the kinetic energy released in the dissociation, $P(E_k)$, is a maximum at $E=0$, and falls off approximately exponentially with a width of about 300 meV [23]. Many GSD events, therefore, result in collision energies that are much lower than can easily be achieved using a merged-beams method, making the GSD process a valuable experimental tool for studies of very slow $H^+ + D(1s)$ collisions. While pure single ionization populates only the $HD^+(1s\sigma)$ ground state, fast proton impact on neutral HD can lead to ionization excitation and double ionization as well. These processes also produce H^+ and D^+ ions, but have kinetic-energy releases much larger than GSD, and are thus experimentally distinguishable. For example, ionization of one electron and excitation of the other to the $2p\sigma$ state will result in a $D^+ + H(1s)$ half collision with a few eV,

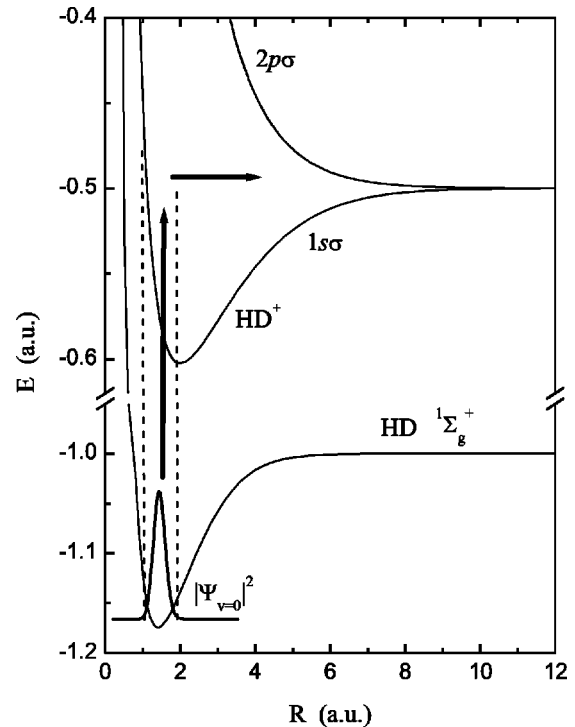


FIG. 2. A schematic view of the GSD process. Ionization of the HD molecule by an incident 4 MeV proton results in vertical transitions to the HD^+ electronic ground state. If the populated $1s\sigma$ vibrational state is in the continuum, a dissociation follows. Charge transfer can then occur during the dissociation. The coupling between the $1s\sigma$ and $2p\sigma$ states is strongest near 12 a.u. [17]. The HD curve is from Ref. [12] and the HD^+ curves from Ref. [13].

much higher in energy than the GSD events of interest.

Experimentally, the procedure is to identify the recoil ion by its mass to charge ratio first, and then determine the half-collision energy *a posteriori* from the measured momentum vector of the dissociating charged fragments for each collision event. The experimental setup is shown in Fig. 3. Since the energy of the GSD fragments is almost always less than 1 eV, cold target recoil ion momentum spectroscopy (COLTRIMS) [25,26] methods are well suited for determination of the fragment momentum. Our apparatus, which was described briefly in previous publications [22–24], uses

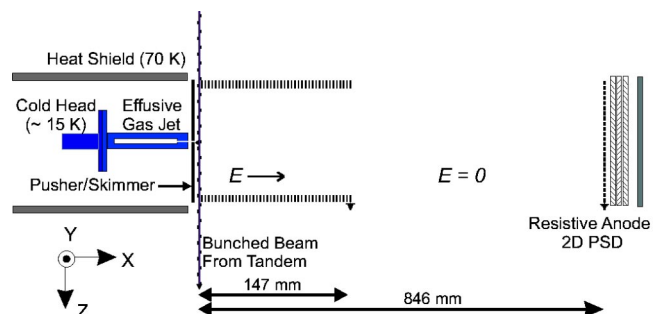


FIG. 3. (Color online) A conceptual drawing of the cylindrically symmetric apparatus. Note the lab-frame coordinate system, which is used throughout this paper.

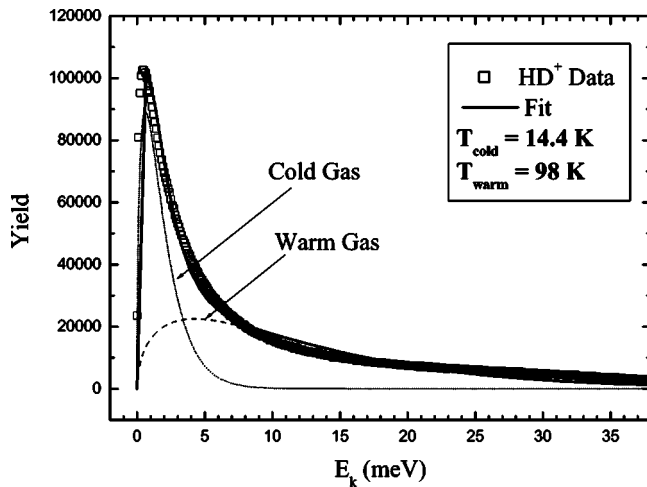


FIG. 4. The measured energy distribution of HD^+ ions produced by 4 MeV proton impact. The temperature of this distribution is determined by fitting it with two Maxwell-Boltzmann distributions. The warm gas and cold gas contributions are approximately equal.

many COLTRIMS techniques. It differs, however, from a traditional transverse extraction COLTRIMS apparatus in two main respects. First, our neutral target does not originate from a supersonic jet aligned perpendicular to both the extraction field and the incident projectile. In our system, HD is precooled to approximately 15 K in a gas cell, and then effuses out of a thin tube (0.3 mm diameter 3.5 mm long) toward the position sensitive detector. This cold gas jet is intersected by a bunched 4 MeV proton beam at a 90° angle. The length to width ratio of the tube is sufficient to collimate the effusive beam of the neutral target somewhat [27] and the flow is further restricted by a 0.5 mm hole in the pusher (and skimmer) plate of the spectrometer, as shown in Fig. 3. The distance from the exit of the gas cell to the interaction point of the neutral and ion beams is approximately 7 mm, and the size of the target at the interaction region is about 1.5 mm. This geometry was selected as a compromise between the experimental need to have a cold localized gas target and the economic need to reduce the use of rather costly HD gas. This geometry leads to the second difference between this apparatus and a typical COLTRIMS apparatus. In our experiment, the ionized electron is not measured, since the effusive jet assembly is located in the space that might be occupied by an electron detector. The temperature of the effusive target is determined by fitting a Maxwell-Boltzmann distribution to the measured HD^+ energy distribution as illustrated in Fig. 4. Our target temperature was determined to be ≈ 15 K using this method.

The charged fragments produced in the collision are extracted by the electrostatic fields of our spectrometer and accelerated toward a two-dimensional position sensitive detector. The detector is used to record both the position and arrival times of the fragments event by event. The proton beam is bunched to widths ranging from 0.8 to 1.2 ns, and the fragment time-of-flight is determined relative to a signal synchronized to the buncher master clock. The beam-bunch repetition rate was selected such that the time between bunches, typically between 10.6 and 84.8 μs , was longer

than the flight times of the ions of interest, i.e., the H^+ and D^+ fragments of HD^+ , and H_2O^+ which indicated the contamination level of residual water vapor in the vacuum system.

From the measured position and time of flight of the fragments, the full three-dimensional momentum vector, and therefore the dissociation energy, was reconstructed. The finite size of the target was corrected by using a weak electrostatic lens [23]. The focusing voltage was selected to obtain the best three-dimensional focus. The time-of-flight resolution was typically 1.6 ns, and was dominated by the 1 ns channel width of the time-to-digital converter and the 1.2 ns beam-bunch width. The resolution of the resistive anode position sensitive detector used was 0.18 mm. The y and z momentum components (note the coordinate system in Fig. 3) were extracted from the position of the fragments on the position sensitive detector. The x component of the momentum was directed along the time-of-flight axis. The conversion to P_x from the time of flight was accomplished by simulating the effects of the extraction field in SIMION [28]. In the simulation, the time of flight was evaluated for ions having a full range of possible P_x values (as expected from theory [17,22]). The simulated time-of-flight dependence on P_x was well described by a second-order polynomial, which was used to convert the measured time of flight to P_x .

The validity of the simulation was verified by the nice agreement between the simulated and measured times of flight of the different species in our target. In general, the difference between the simulated and measured times of flight was better than 1–3 ns out of total flight times of at least 1 μs , and often more than 10 μs (a relative error of 0.1%). While the differences between experimental and simulated time of flight are comparable to the error in the time-of-flight measurement, it is the difference in the time of flight from the peak centroid, $t(v_x) - t(v_x=0)$, that is needed to evaluate P_x . The error in this quantity is much smaller as most sources of error affect both $t(v_x)$ and $t(v_x=0)$ equally, and the errors cancel upon subtraction. At low extraction fields, many GSD fragments had enough kinetic-energy release to strike the spectrometer pusher or skimmer plate. As a result, only half of the momentum distribution (GSD fragments with an initial velocity toward the position sensitive detector) are used for the results shown in the following section. In addition, GSD fragments with positive initial velocity were unaffected by small spectrometer field distortions near the 0.5 mm hole in the skimmer or pusher plate.

Determination of the D^+ yield and, hence, the charge-transfer probability, is complicated by the presence of H_2 in the target. We have developed and previously reported on two reliable methods for measuring the level of this H_2 contamination in the HD target [23]. Briefly, the H_2^+ contamination level is determined by separating the H_2^+ molecular ions from D^+ GSD fragments by differences in momentum, or by careful analysis of the time-of-flight spectrum from a HD target and theoretical knowledge of the GSD fractions based on Franck-Condon calculations [23]. For the current experiment, however, this is not enough, since the quantity of interest is the D^+ yield as a function of E_k . One approach

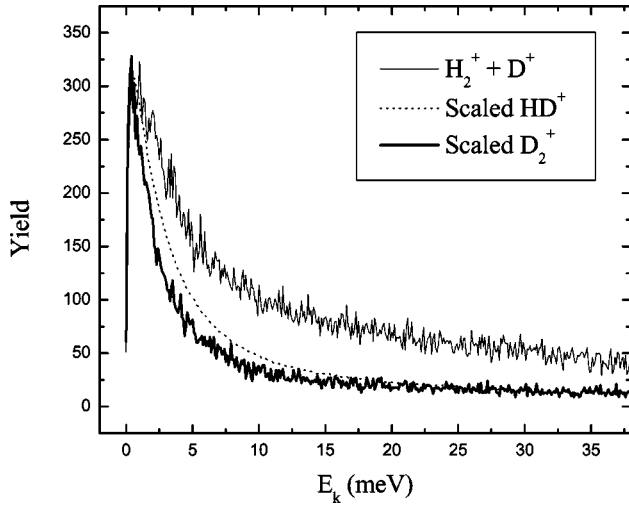


FIG. 5. The measured energy distributions for H_2^+ , HD^+ , and D_2^+ after single ionization by 4 MeV protons. The heavier D_2^+ ions have a narrower energy distribution, while the lighter H_2^+ ions have the widest distribution. The reason for the different width distributions remains undetermined.

to this problem was to use the abundant HD^+ events collected in the experiment as a high precision simulation of the $\text{H}_2^+(E_k)$ population [22]. Since the H_2 , HD , and D_2 molecules in the target all came from the effusive jet, and therefore the same heat reservoir, it seemed reasonable to expect that the energy distributions of the HD^+ and H_2^+ populations would be identical. As shown in Fig. 5, however, the various isotopes had a slightly different distribution at low energies. While this made very little difference in the charge-transfer measurement above ≈ 40 meV, near threshold it proved problematic. The HD^+ population was too narrow to correctly simulate the H_2^+ distribution, leading to a systematic over subtraction from the $D^+(E_k)$ population near threshold.

The difference in energy distribution might be related to the momentum transferred to the molecule in the ionization process. If the momentum transfer is photoionization-like, (that is, equally balanced between the electron and recoil ion) as has been observed for similar collisions in which the projectile has a low z/v [25,31], the resulting recoil energy distribution should be narrower for heavier targets. A simple scaling based on this assumption, however, does not entirely account for the differences seen in Fig. 5. A second possibility is that the flow from the effusive jet is somewhat mass dependent. This would most likely be the case if the pressure in the cooling cell was high enough that molecular flow could not be assumed. Measurements of the inlet gas pressure would seem to indicate that assuming molecular flow is valid, but a systematic study of the energy distribution as a function of driving pressure has not been carried out to date.

Whatever the cause of the difference in the energy distributions, we have adopted another approach to determine the yield of H_2^+ as a function of energy. Since the relative amounts of H_2 and HD can be well established by our previous methods [23], we simply conduct a separate measurement with a pure H_2 target to determine the energy distribu-

tion. Some care must be taken to ensure the experimental conditions are the same between the runs with the HD and H_2 targets, since the measurement is sensitive to small changes in the temperature of the target and the spectrometer voltages. Once the H_2^+ energy distribution is obtained, the yield is normalized to the level of the H_2^+ contamination in the HD target using previous methods [23] and the H_2^+ contamination is subtracted from the $D^+(E_k)$ measurement. This brings the measured threshold significantly closer to the expected threshold than in our previous publication [22]. As we will discuss in the next section, however, some discrepancy still exists.

Details on several other experimental considerations, including detection efficiency, subtraction of contributions to the $m/q=1$ and 2 channels from residual water vapor in the target, and limiting chemical reactions of the dissociating fragments with the residual gas, may be found in our earlier publications [22–24].

III. RESULTS AND DISCUSSION

Denoting the measured yields of the GSD events as $H^+(E_k)$ and $D^+(E_k)$, the probability for charge transfer is given by

$$P_t(E_k) = \frac{D^+(E_k)}{H^+(E_k) + D^+(E_k)} = \frac{\sigma_t}{\sigma_e + \sigma_t}, \quad (1)$$

where σ_e and σ_t are the theoretically computed values for $H^+(E_k)$ and $D^+(E_k)$ production, respectively [23]. While $P_t(E_k)$ is typically expressed in terms of the S -matrix element, Eq. (1) has the advantage of allowing a direct comparison between experiment and theory. Similarly, the probability for elastic scattering is

$$P_e(E_k) = \frac{H^+(E_k)}{H^+(E_k) + D^+(E_k)} = \frac{\sigma_e}{\sigma_e + \sigma_t}. \quad (2)$$

Finally, the ratio of the bound-free transitions to total single ionization, calculated from the Franck-Condon factors, can be expressed as

$$P(E_k) = \frac{H^+(E_k) + D^+(E_k)}{\sigma^+} = \frac{H^+(E_k) + D^+(E_k)}{HD^+ + H^+ + D^+}, \quad (3)$$

where σ^+ is the pure single-ionization cross section [ionization to the $\text{HD}^+(1s\sigma)$ ground state] and HD^+ is the measured yield of HD^+ molecular ions.

The factors contributing to the uncertainty in determining the kinetic-energy release E_k can be grouped into two categories. The first type includes factors that influence the center-of-mass motion of the HD^+ ion. Thermal motion adds an energy spread of 1.2 meV at the temperature (14.4 ± 2.1 K) of our precooled gas target. The recoil energy imparted to the HD^+ ion during the vertical ionization also adds to the center-of-mass motion of the HD^+ ion. We could not find any experimental data for the recoil momentum distribution in our collision system ($4 \text{ MeV } \text{H}^+ + \text{HD} \rightarrow \text{H}^+ + \text{HD}^+ + e^-$), but we can estimate the value from slightly different collision systems. Extrapolating the results of Tobu-

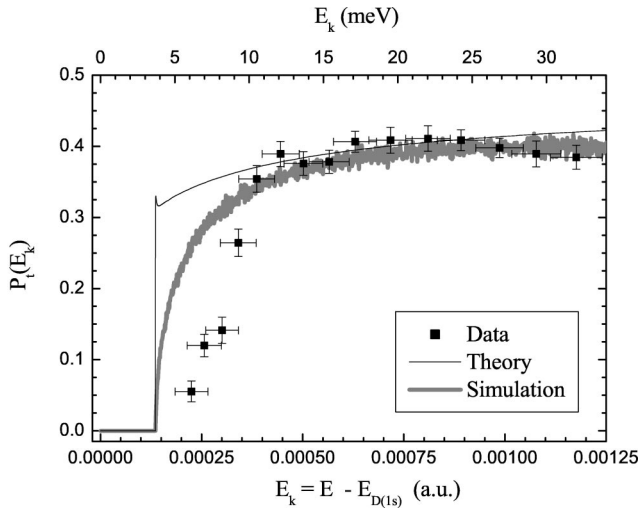


FIG. 6. Experimental results for the charge-transfer (P_t) channel as a function of E_k . E_k is measured relative to the $D(1s)$ threshold. Also plotted are the theoretical calculations [22]. The thick line shows the results of a simulation used to convolute the theoretical results with the factors affecting the experimental resolution.

ren and Wilson [29] to lower collision energies gives a recoil momentum distribution with a full width at half maximum (FWHM) of ~ 0.11 a.u. Using the very low-energy values of Tribedi *et al.* [30] and merging those results with the higher-energy measurements of Toburen and Wilson yields a FWHM of ~ 1 a.u. In addition, measurements of ionization in the 4 MeV $H^+ + He$ collision system reveal a momentum distribution of ≈ 0.5 a.u. [31], in between the previous two estimates. The second category of factors influencing the energy resolution are related to the measurement technique itself, including the position and timing resolution, discussed in Sec. II.

Previously, we have reported measurements of $P_t(E_k)$ with E_k ranging from threshold to nearly 1 eV [22]. This paper will focus on measurements near the threshold for charge transfer. Our measurement of $P_t(E_k)$ is shown in Fig. 6. The experimental results are compared to coupled-channel scattering calculations. The scattering calculations, based on the adiabatic potentials calculated by Esry and Sadeghpour [13], were initially done for the full-collision problem [17]. The calculations were then modified to fit the current half-collision problem [22]. The modifications were needed to account for the Franck-Condon transition from the neutral molecule as well as the target temperature. Projecting the ground state of the neutral HD molecule onto the continuum states of HD^+ [23] links the results of the coupled-channels scattering problem with the vertical ionization process. The target temperature of less than 20 K means our calculations need only include $J=0$, since it is essentially the only rotational state initially populated at that temperature. Much of the structure seen in the full-collision calculations is not present in the current calculations, since that structure arises from shape resonances for $J \geq 10$ [17]. Our measurements show good agreement with the coupled-channel calculations for the energy range measured, with the exception of the

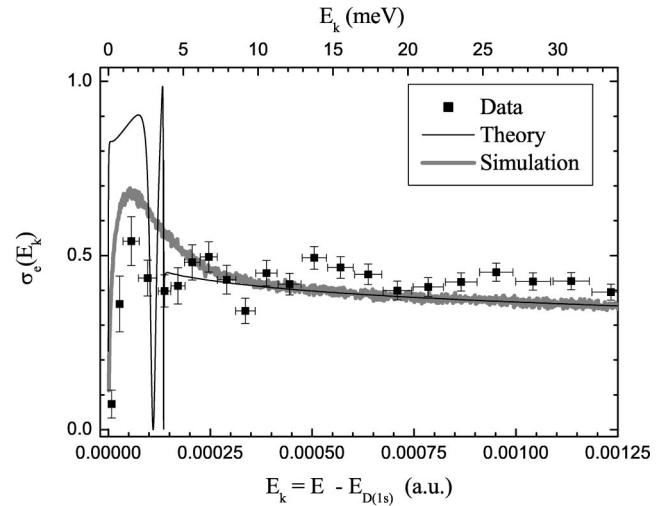


FIG. 7. Experimental results for the elastic-scattering (σ_e) channel as a function of E_k . Theoretical results [22], and those results convoluted with the experimental resolution are shown in a manner similar to Fig. 6.

threshold behavior. The theoretical predictions are also convoluted with the experimental resolution using a simulation (described below), but this does not account for the difference between theory and experiment near threshold. This disagreement is most likely due to a systematic error in subtracting the H_2^+ contamination from the target at very low energies. As noted previously, and shown in Fig. 5, the isotopic difference in measured energy distributions leads to an over subtraction of the H_2^+ contamination near threshold. This systematic error is caused by differences in the shape of the actual energy distribution of H_2^+ with respect to the distribution we used to subtract background from the data. The error is not due to any error in estimating the magnitude of the H_2 contamination. This systematic error is large enough to account for all of the ≈ 3 meV offset between theory and experiment near threshold in Fig. 6. This problem is localized near threshold, and for $E_k > 10$ meV, the energy distribution of H_2^+ is well determined, thus resulting in a minimal effect. Coincident measurement of the momentum of the ionized electron or a careful study of any mass-dependent effects in the velocity distribution of the effusive jet might resolve this systematic error.

For the elastic channel, it is more convenient for us to compare

$$\sigma_e = P_e(E_k)P(E_k) = \frac{H^+(E_k)}{\sigma^+}, \quad (4)$$

to theory since Eq. (4) does not contain the problematic D^+ channel. In contrast to the charge-transfer channel, which showed no resonance structure, our calculations for the elastic channel show two $J=0$ Feshbach resonances located below the threshold for charge transfer [22]. The experimental results for this elastic channel are shown in Fig. 7. Again, we find theory and experiment to be in good agreement.

It is important to note that Figs. 6 and 7 represent a direct comparison, described in Eqs. (1) and (4), between theory and experiment, without the need to scale by some arbitrary factor. The half-collision calculations that complement this experiment [22] are identical to the calculations done for a full-collision system [17] except for the need to incorporate the vertical transition from the neutral HD molecule, and therefore these experimental results represent the first direct test of theory in this very low-energy range. These results demonstrate the feasibility of using the GSD process to study this basic ion-atom collision at energies much lower, and with better resolution, than presently possible using traditional merged-beams techniques. The current experiment lacks the resolution, however, to map the structure caused by the Feshbach resonances in the elastic channel. This is unfortunate, since a measurement of the resonance locations would be a very useful test of theory, as this method is more stringent than comparing total cross sections [17].

IV. FUTURE DEVELOPMENTS

Is it possible to improve the experimental resolution enough to map the resonance structure in the elastic channel? To investigate this question, we have constructed a simulation to investigate how the various factors leading to uncertainty in the measured KER propagate in the measurement and affect the ultimate resolution of the experiment. The simulation convolutes the theoretically predicted charge-transfer and elastic-scattering probabilities with the detection (position and TOF) resolution of the GSD fragments, the center-of-mass thermal motion of the HD target, the center-of-mass recoil during the ionization process, and the possibility of a systematic shift in the centroid of the D^+ TOF peak. Besides the theoretical charge-transfer and elastic-scattering probabilities, the inputs to the program include the TOF centroids for the H^+ and D^+ peaks, the spectrometer geometry, and the two coefficients of the second-order polynomial used in the conversion of fragment time of flight to P_x . For each simulated E_k value, a molecular orientation is chosen using a Monte Carlo approach. Isotropic angular distribution is assumed for the GSD process. The simulated TOF and position of impact on the detector are calculated based on the spectrometer geometry. The different sources of E_k broadening are then added to these values, and the resulting E_k is binned into an equally spaced energy spectrum, just as in the actual measurement.

If only the energy broadening due to detection resolution is included in the simulation, the structure associated with the two Feshbach resonances in the elastic channel is still quite noticeable. When the center-of-mass broadening is added into the simulation, the resonance structure disappears. Our experimental results for the elastic channel are in good agreement with the simulation, especially if the recoil momentum distribution is assumed to have a FWHM near 1 a.u., which is on the larger side of the estimates discussed above. In the charge-transfer channel, the experimental results have the shape predicted by the simulation, but appear to be shifted by 2 to 3 meV from the expected value. This shift is most likely related to a remaining systematic error in

the subtraction of the H_2^+ contamination. The simulation shows conclusively that most of the E_k broadening is due to uncertainties in the center-of-mass motion of the HD^+ target.

For the present experimental setup, the factors affecting the center-of-mass motion of the HD target are fixed. A different experimental design, allowing for additional geometric cooling of the target and coincident detection of the ionized electron, could improve the energy resolution by reducing these sources of broadening. Rotating the jet so it is perpendicular to both the time-of-flight and ion-beam axis would allow for the location of an electron detector opposite to the recoil ion detector. This standard COLTRIMS configuration [25,26] would allow the recoil momentum distribution to be measured, reducing the uncertainty in the center-of-mass motion of the HD target. In addition, the temperature of the HD target could be further reduced using a precooled supersonic gas jet with multiple (usually two) molecular beam skimmers. Such a configuration has yielded target temperatures of 77 mK [26]. Furthermore, the presence of two or more skimmers reduces the “hot gas” contamination in the target to negligible levels. The simulated results for σ_e under these experimental conditions are shown in Fig. 8. The dip in the cross section associated with the first Feshbach resonance is clearly visible.

The price for such an improvement is the conversion from an economical effusive jet that was located within 1 cm of the interaction region to a more expensive multiple stage supersonic jet. Deuterium hydride gas is costly, with a supersonic jet of the type described above estimated to use more than \$10k/day. A more economical alternative might be reducing the number of skimmers and, thereby, reducing the gas consumption. To estimate the resolution that could be obtained with such a configuration, we note that Wu *et al.* [32] introduced a single skimmer to improve their transverse momentum resolution by $\sim 6\times$ over the experiments of Frohne *et al.* [33] and Ali *et al.* [34], who used effusive jet sources similar to the current apparatus. Using this enhancement in resolution to estimate the expected improvement in our current source yields a target temperature of 5 K. In addition, a single skimmer does not reduce the hot gas contamination as effectively. Based on the experience of Landers [31] with a single-skimmer jet, we estimate that about 30% of the target will be hot gas. When using these estimates as inputs for the simulation, the simulated σ_e results are able to marginally resolve the Feshbach resonance location, as shown in Fig. 8. The improvements discussed above will also improve our ability to probe the threshold behavior of the charge-transfer channel, as shown in Fig. 9. The simulated results shown in Fig. 9 assume that the systematic error in the subtraction of the H_2 contamination is overcome. Currently, however, the H_2 contamination remains the largest obstacle to probing the threshold region in this channel.

Beyond this measurement, the GSD process can be used as a sensitive probe in other ion-molecule collisions. Measuring the momentum vector of the dissociating fragments allows *a posteriori* determination of the molecular alignment at the time of the collision. Anisotropies of angular distributions of H_2 dissociation products have been studied for

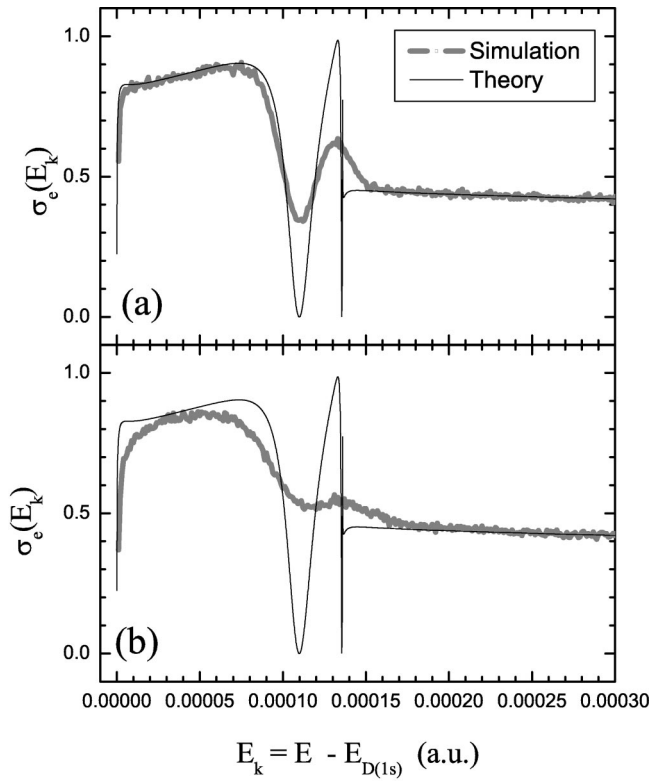


FIG. 8. Theoretical predictions for σ_e [22] and the expected experimental results with an improved apparatus. Expected results from a state-of-the-art two-stage supersonic jet and COLTRIMS apparatus are shown in (a), while a jet configuration with more economic HD consumption are shown in (b). The target temperature in (a) is 77 mK, while in (b) it is 5 K. Warm gas (100 K), accounts for 5% of the target in (a) and 30% in (b). Mapping the resonance locations seems possible using (a), while (b) seems marginal. Both (a) and (b) assume the detection of the ionized electron to measure the recoil momentum imparted to the HD^+ molecular ion during the collision.

nearly seven decades [35]. Dunn described general rules for transition probabilities between pairs of electronic states for H_2 collisions with electrons [36,37]. Dissociative ionization, however, predominantly occurs from excited electronic states, complicating the analysis. Focusing on the GSD channel allows measurements of the angular distribution of the pure single-ionization channel alone, a significant experimental improvement. Analysis of the present data as a function of molecular alignment shows little anisotropy. The present measurement, however, is compromised by the rather large amount of hot gas in our target. Improving the apparatus to reduce the hot gas, as discussed earlier in this paper, would improve this measurement considerably.

Recent measurements of electrons ionized in 60 MeV/u $Kr^{34+} + H_2$ collisions reveal oscillations in the electron emission cross section resulting from interference effects analogous to Young's double slit experiment [38]. These measurements are integrated over the molecular orientation, and considerable analysis was required to uncover the oscillations in the cross section. Measurements of the GSD fragments in coincidence with the electrons would eliminate the

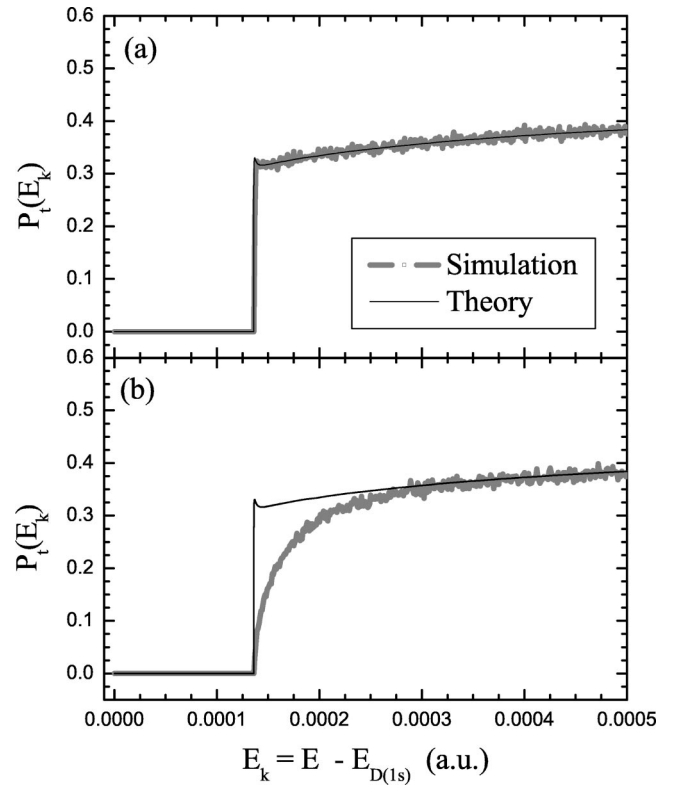


FIG. 9. Similar to Fig. 8 except for the charge-transfer channel.

need to integrate over the molecular orientation. In addition, the GSD process is clearly associated with single ionization to a well-defined final state, further simplifying the problem. As a practical matter, the collection of 50–100 eV electrons (which have a de Broglie wavelength similar to the internuclear distance of H_2) in coincidence with GSD fragments below 1 eV is nontrivial, but could conceivably be accomplished by a COLTRIMS apparatus with a pulsed extraction field or a spectrometer with multiple extraction and acceleration regions.

In slow ion-molecule collisions, the GSD process has proved useful in separating the momentum transferred to the center-of-mass motion of the molecular target from the momentum imparted to internal motion of the nuclei. Since the GSD fragments are very slow, they are sensitive probes of the momentum transfer. This technique, when applied to slow ($v \leq 0.5$ a.u.) $He^+ + H_2$ collisions, has shown that ionization transfers some momentum to the internal motion of the nuclei, while the electron capture process does not [39].

V. SUMMARY

We have developed a method for studying very slow collisions between a proton and a deuterium atom. This method utilizes the ground-state dissociation of $HD^+(1s\sigma)$ to produce very slow $H^+ + D(1s)$ half collisions. Momentum imaging of the dissociating charged GSD fragments is used to determine the collision energy. We have extended the energy range down by more than one order of magnitude and obtain much better energy resolution than is presently possible in merged-beams experiments. These experimental re-

sults provide a direct test of half-collision scattering calculations. Since our half-collision calculations were done using the same techniques as for the full-collision problem [17], our results provide an experimental test of the theory for this fundamental, very slow, ion-atom collision system. Simulations indicate that, with some apparatus modification to obtain better momentum resolution, this technique should be able to probe the location of Feshbach resonances in the elastic-scattering channel, an even more stringent test of theory than the current results. Finally, the very slow GSD fragments are sensitive probes of molecular alignment and momentum transfer in ion-molecule collisions, and we de-

scribe several measurements that further utilize the GSD process.

ACKNOWLEDGMENTS

The authors would like to thank B. D. Esry and H. R. Sadeghpour for their work on the calculations [13,17,22] that complement this measurement and A. L. Landers for useful discussions about the interference phenomena [38] discussed in Sec. III. This work was supported by the Chemical Sciences, Geosciences, and Biosciences Division, Office of Basic Energy Sciences, Office of Science, U.S. Department of Energy.

-
- [1] R.C. Isler, *Plasma Phys. Controlled Fusion* **36**, 171 (1994).
 [2] M.A. Lieberman and A.J. Lichtenberg, *Principles of Plasma Discharges and Materials Processing* (Wiley, New York, 1994), pp. 73-77.
 [3] R.R. Hodges, Jr. and E.L. Breig, *J. Geophys. Res., [Space Phys.]* **96**, 7697 (1991); **98**, 1581 (1993).
 [4] S.A. Fuselier, E.G. Shelley, B.E. Goldstein, R. Goldstein, and M. Neugebauer, *Astrophys. J.* **379**, 734 (1991).
 [5] P.C. Stancil, S. Lepp, and A. Dalgarno, *Astrophys. J.* **509**, 1 (1998).
 [6] A. Dalgarno and H.N. Yadav, *Proc. Phys. Soc. Jpn.* **66**, 173 (1953).
 [7] H.D. Gilbody, *Adv. At., Mol., Opt. Phys.* **33**, 149 (1994).
 [8] J.H. Newman, J.D. Cogan, D.L. Zeigler, D.E. Nitz, R.D. Rundel, K.A. Smith, and R.F. Stebbings, *Phys. Rev. A* **25**, 2976 (1982).
 [9] A.V. Matveenko, *J. Phys. B* **10**, 1133 (1977).
 [10] G. Hunter and M. Kuriyan, *Proc. R. Soc. London, Ser. A* **245**, 175 (1978).
 [11] J. Davis and W.R. Thorson, *Can. J. Phys.* **56**, 996 (1978).
 [12] W. Kołos, K. Szalewicz, and H.J. Monkhorst, *J. Chem. Phys.* **84**, 3278 (1986).
 [13] B.D. Esry and H.R. Sadeghpour, *Phys. Rev. A* **60**, 3604 (1999).
 [14] J. Macek and K.A. Jerjian, *Phys. Rev. A* **33**, 233 (1986).
 [15] R.E. Moss and I.A. Sadler, *Mol. Phys.* **61**, 905 (1987).
 [16] A. Igarashi and C.D. Lin, *Phys. Rev. Lett.* **83**, 4041 (1999); **86**, 747 (2001).
 [17] B.D. Esry, H.R. Sadeghpour, E. Wells, and I. Ben-Itzhak, *J. Phys. B* **33**, 5329 (2000).
 [18] A.V. Matveenko, *Phys. Rev. Lett.* **86**, 746 (2001).
 [19] D. Galli and F. Palla, *Astron. Astrophys.* **335**, 403 (1998).
 [20] D.W. Savin, *Astrophys. J.* **566**, 599 (2002).
 [21] S. Lepp, P.C. Stancil, and A. Dalgarno, *J. Phys. B* **35**, R57 (2002).
 [22] E. Wells, K.D. Carnes, B.D. Esry, and I. Ben-Itzhak, *Phys. Rev. Lett.* **86**, 4803 (2001).
 [23] E. Wells, B.D. Esry, K.D. Carnes, and I. Ben-Itzhak, *Phys. Rev. A* **62**, 062707 (2000).
 [24] I. Ben-Itzhak, E. Wells, K.D. Carnes, Vidhya Krishnamurthi, O.L. Weaver, and B.D. Esry, *Phys. Rev. Lett.* **85**, 58 (2000).
 [25] M.A. Abdallah, A. Landers, M. Singh, W. Wolff, H.E. Wolf, E.Y. Kamber, M. Stöckli, and C.L. Cocke, *Nucl. Instrum. Methods Phys. Res. B* **154**, 73 (1999).
 [26] R. Dörner, V. Mergel, O. Jagutzki, L. Spielberger, J. Ullrich, R. Moshammer, and H. Schmidt-Böcking, *Phys. Rep.* **330**, 95 (2000).
 [27] H. Pauley, in *Atomic and Molecular Beam Methods*, edited by G. Scoles (Oxford University Press, New York, 1988), Vol. 1, pp. 87-92.
 [28] D.A. Dahl, Computer Code SIMION version 6.0 (Lockheed Martin Idaho Technologies, Idaho National Engineering Laboratory, Idaho Falls, ID, 1995).
 [29] L.H. Toburen and W.E. Wilson, *Phys. Rev. A* **5**, 247 (1977).
 [30] L.C. Tribedi, P. Richard, L. Gulyas, and M.E. Rudd, *Phys. Rev. A* **63**, 062724 (2001).
 [31] A.L. Landers, Ph.D. thesis, Kansas State University, Manhattan, Kansas, 1999.
 [32] W. Wu, J.P. Giese, Z. Chen, R. Ali, C.L. Cocke, P. Richard, and M.P. Stöckli, *Phys. Rev. A* **50**, 502 (1994).
 [33] V. Frohne, S. Cheng, R. Ali, M. Raphaelian, C.L. Cocke, and R.E. Olson, *Phys. Rev. Lett.* **71**, 696 (1993).
 [34] R. Ali, V. Frohne, C.L. Cocke, M. Stöckli, S. Cheng, and M.L.A. Raphaelian, *Phys. Rev. Lett.* **69**, 2491 (1992).
 [35] V.N. Sasaki and T. Nakao, *Proc. Imp. Acad. Japan* **11**, 138 (1935).
 [36] G.H. Dunn, *Phys. Rev. Lett.* **8**, 62 (1962).
 [37] G.H. Dunn and L.J. Kieffer, *Phys. Rev.* **132**, 2109 (1963).
 [38] N. Stolterfoht, B. Sulik, V. Hoffmann, B. Skogvall, J.Y. Chesnel, J. Rangama, F. Frémont, D. Hennecart, A. Casimi, X. Husson, A.L. Landers, J.A. Tanis, M.E. Galassi, and R.D. Rivarola, *Phys. Rev. Lett.* **87**, 023201 (2001).
 [39] W. Wolff, I. Ben-Itzhak, H.E. Wolf, C.L. Cocke, M.A. Abdallah, and M. Stöckli, *Phys. Rev. A* **65**, 042710 (2002).